J Solid State Electrochem (1998) 2: 347–354

ORIGINAL PAPER

Marcin Opallo

Electrochemical redox reactions studied in frozen tetrabutylammonium halide hydrates

Received: 16 December 1997 / Accepted: 10 February 1998

Abstract The electrochemical redox reactions: $Fe(CN)_6^{4-} - e^- \leftrightarrow Fe(CN)_6^{3-}$, $Ru(NH_3)_6^{3+} + e^- \leftrightarrow Ru(NH_3)_6^{2+}$ and $Fc(CH_2OH)_2 - e^- \leftrightarrow Fc(CH_2OH)_2^+$ (Fc–ferrocene) were investigated in tetrabutylammonium halide hydrates at temperatures below and above the electrolyte melting point. They were studied by cyclic voltammetry, potential step chronoamperometry and impedance spectroscopy. Freezing of the electrolyte affects both the shape and position of the cyclic voltammogram on the potential scale. Also the shapes of the current-time relationship and the impedance spectra change at temperatures below the melting point. It has been proposed that this behaviour is caused by slow transport of the reactant and the heterogeneous nature of the electrolyte. The activation energies of reactant transport are about four times larger in frozen electrolytes than those in liquid. It has been concluded that reactant transport is restricted to the intergrain space of the electrolyte.

Key words Electrode reactions · Frozen electrolyte · Chronoamperometry · Impedance spectroscopy · Ultramicroelectrodes

Introduction

Studies of simple electrode reactions at temperatures below the melting point of stoichiometric electrolytes have recently been undertaken [1–8]. These offer the unique opportunity to investigate an electrode reaction in the same electrolyte in different physical states. It was observed that the transport of reactant in frozen electrolyte is much slower than in liquid [1–8]. Correspondingly, the activation energy of this process substantially increases at temperatures below the melting point of the electrolyte [2, 4, 6]. It was also concluded that, contrary to the situation in a liquid electrolyte, the volume available for reactant motion in a frozen electrolyte is probably restricted to the intergrain space of the electrolyte [4–6]. Freezing of the electrolyte also affects the electrochemical stability of redox-active ions and molecules [3, 6, 7]. The temperature dependence of the redox potential is generally more pronounced at temperatures below the melting point of the electrolyte, indicating that freezing of an electrolyte enhances the electrochemical stability of the redox form with the larger absolute value of electric charge [3, 6, 7].

The electrochemical redox systems studied in frozen electrolyte were mainly $Fe^{3+/2+}$ in $HClO_4 \cdot 5.5\ H_2O$ [1, 2] and $Fe(CN)_6^{3-/4-}$ in tetraalkylammonium salts and hydroxide hydrates [3–8]. This was because of the limited stability and/or solubility of other redox-active ions or molecules in these electrolytes due to extreme pH values. A larger variety of redox systems can be examined in tetrabutylammonium halide hydrates. The faradaic signal connected with the electrochemical redox reaction of added redox-active ions or molecules can be observed in a limited temperature range below the melting point of $(C_4H_9)_4NF \cdot 32H_2O$ (TBAF32) [3]. The electrochemical stability of redox-active ions and molecules in tetrabutylammonium halide hydrates was also recently studied [7].

The aim of this work is to investigate how the freezing of tetrabutylammonium halide hydrates affects the mechanism of electrode reactions of different redox-active ions and molecules. Three electrode reactions, involving an anionic, a cationic and a neutral molecule respectively were selected:

$$Fe(CN)_6^{4-} - e \longleftrightarrow Fe(CN)_6^{3-} \quad (1)$$

$$Ru(NH_3)_6^{3+} + e \longleftrightarrow Ru(NH_3)_6^{2+} \quad (2)$$

$$Fc(CH_2OH)_2 - e \longleftrightarrow Fc(CH_2OH)_2^+ \quad (3)$$

Marcin Opallo (✉)
Institute of Physical Chemistry, Polish Academy of Sciences, ul.Kasprzaka 44/52, 01-224 Warsaw, Poland
Fax: +48-3912-0238; e-mail: mopallo@ichf.edu.pl

As electrolytes, the following tetrabutylammonium cation halide hydrates [9, 10] were selected: $(C_4H_9)_4NF \cdot 32H_2O$ (TBAF32), $(C_4H_9)_4NCl \cdot 30H_2O$ (TBACl30) and $(C_4H_9)_4NBr \cdot 32H_2O$ (TBABr32). These melt congruently at 301 K, 287 K and 287 K respectively [9, 10]. It has been shown that all these compounds are normal ionic conductors [11].

An experiment with an electrochemical system modelling the frozen electrolyte with redox-active ions [6] was also performed.

Experimental

Chemicals

$K_3Fe(CN)_6 \cdot 3H_2O$, $K_4Fe(CN)_6$ (POCh, analytical grade) and $Ru(NH_3)_6Cl_3$ (Sigma) were used without further purification. $Fc(CH_2OH)_2$ (Aldrich) was recrystallized from heptane. Tetrabutylammonium halide hydrates were obtained from the corresponding halides: TBAF (Jannsen Chimica), TBACl (Fluka) and TBABr (Fluka), according to a procedure described in [9]. The 0.5–2 M aqueous solution of the corresponding halide was left overnight at a temperature of 278 K. The solid precipitate was collected and recrystallized from water at the same temperature. The purity of a given hydrate was checked by melting point measurements. Its stoichiometry was also confirmed by comparison of the ^2H NMR signal of butyl and water deuterons. $TBA_3Fe(CN)_6$ was obtained by the reaction of stoichiometric amounts of $K_3Fe(CN)_6$ and TBAF in CH_2Cl_2 as described in [12]. The stoichiometry of the product was confirmed by elemental analysis: calculated C 69.05%, H 11.59% and N 13.42%, and obtained C 68.61%, H 11.41% and N 13.21%.

The water used in the electrolyte preparation was quadruply distilled, the last two times from quartz. Pure argon was used for deareation of electrolytes.

Apparatus and methods

Reactions 1–3 were studied by cyclic voltammetry and potential step chronoamperometry. The potential sweep and potential step experiments were performed using the Autolab (Eco Chemie) electrochemical system. The data were acquired and analyzed using GPES software. These experiments were done in a three-electrode cell with a Pt disc as the working ultramicroelectrode ($d = 20$ μm), with Pt wire as the counter electrode and a tungsten oxidized wire reference electrode [13, 14]. The reference electrode was prepared from freshly cut and cleaned 1-mm diameter tungsten wire. It was kept for 3–4 days in electrolyte solution until its potential became stable within a few millivolts. The temperature coefficient of the reference electrode in the studied electrolyte is smaller than 0.002 V K^{-1} [7].

Reaction 1 was also studied by impedance spectroscopy. The impedance spectra of the cell: Au | $K_3Fe(CN)_6$ and $K_4Fe(CN)_6$, electrolyte (liquid and frozen) | Au were obtained using the system consisting of a 1260 Impedance/Gain-Phase Analyzer and a 1286 Electrochemical Interface, both from Solartron Instruments. Experimental parameters and data aquisition were controlled by electrochemical impedance software ZPlot for Windows (Scribner Associates). The amplitude of the sinusoidal signal of frequency in the range 10^{-1} to 10^5 Hz was between 5 and 50 mV for higher and lower temperatures respectively. During impedance measurements the cell was kept at a potential equal to rest potential, measured at the beginning of the experiment, typically between 0.001 and −0.01 V.

In all experiments the cell was filled with 3–4 cm^3 of a 1–5×10^{-3} M solution of redox reactant in a given electrolyte. It was placed in the cylindrical chamber of the copper block. This block was installed in a Dewar flask filled with liquid nitrogen or a dry ice/acetone mixture. The temperature of the cell was adjusted by means of heat liberated from a resistive wire placed inside the bottom of the cell block. It was controlled by a temperature controller (type 680, Unipan-Thermal) connected to a Pt100 sensor (Heraeus) placed inside the wall of the copper block. The temperature of the electrolyte was measured using another Pt100 sensor placed in the electrochemical cell and connected to a digital thermometer (EMT-10). The temperature of the cell ranged from 220 to 350 K and the accuracy of temperature measurements was better than 1 K.

All experiments were done in a heating cycle. The temperature of the cell was changed at a rate smaller than 1 K min^{-1}. At the beginning the temperature was lowered to the lowest temperature studied. Before a given measurement, the cell was kept for at least 10 min at constant temperature to allow thermal equilibration.

The experiments with a model bead system were performed in the cell similar to that described in literature [15]. Two Au discs, 1 mm in diameter, embedded in Teflon, served as the top and bottom of a cylindrical Teflon cell. The cell was filled with beads 2×10^{-5} m in diameter of RP-18 soaked in 0.001 M $K_3Fe(CN)_6$ and $K_4Fe(CN)_6$ (1 : 1) solution in liquid TBACl30. During the experiments, a constant pressure was applied to the upper side of the cell, by a 2-kg lead brick.

Other details of the cell, electrodes pretreatment and procedures have been previously described [3–5].

Results and discussion

Cyclic voltammetry

For all systems studied, the shape of the cyclic voltammograms obtained with ultramicroelectrodes and their position on the potential scale depend on the temperature, as previously observed [3, 7].

At temperatures above the melting point of the electrolyte, the shape of the cyclic voltammograms is sigmoidal, typical for near steady state behaviour (Fig. 1). The difference between the one-quarter and the three-quarter wave potentials ($E_{¼}$–$E_{¾}$) is equal to 0.055–0.060 V. This means that this is a reversible one-electron transfer reaction with predominantly radial diffusion to the electrode surface [16]. The plateau current is 6 to 8 times lower than expected on the basis of the literature

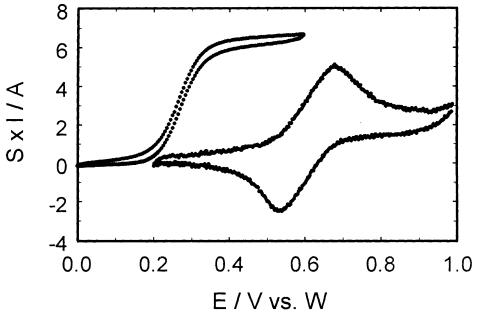

Fig. 1 The cyclic voltammograms recorded in 0.002 M $Fc(CH_2OH)_2$ in TBACl30 at Pt microelectrode ($d = 20$ μm) at temperatures above (290 K sigmoidal voltammogram, $S = 10^9$) and below (245 K, peak-shaped voltammogram, $S = 10^{12}$) electrolyte melting point. Scan rate 0.01 V s^{-1}

value of the diffusion coefficients of the reactants [17, 18]. Adsorption of TBA^+ cations on the electrode surface [19] and aggregation of the electrolyte [20] were proposed previously as the reason for this effect [3].

Voltammograms obtained at temperatures below the melting point of the electrolyte are peak shaped, with similar magnitudes of anodic and cathodic peak currents (Fig. 1). This indicates that in these conditions linear diffusion towards the electrode surface dominates. One may calculate that, for the size of the ultramicroelectrode used, such a change of the shape of the cyclic voltammogram is to be expected when the diffusion coefficient becomes smaller than 10^{-10} m^2 s^{-1}. This effect, together with the observed much smaller current, indicates slower reactant transport towards the electrode surface in the frozen electrolyte, which is in agreement with previous findings [1–6, 8].

Chronoamperometry and apparent diffusion coefficients

The cathodic and anodic current-time dependences obtained from potential step experiments are symmetric at temperatures above and below the melting point, as expected in the case of a reversible electrochemical redox reaction. One may analyse them using a Cottrell plot (I vs $t^{-0.5}$ relationship, where I is current and t time). At temperatures above the melting point of the electrolyte, these plots are linear with a non-zero intercept as expected in the case of radial diffusion [16, 17] (Fig. 2a). One may estimate the diffusion coefficients D_{app} of the reactants from the value of the limiting steady-state current I_1 using the following equation [17]:

$$I_1 = 4nFD_{app}cr \quad (4)$$

where c is the reactant concentration, r is the electrode radius, n is the number of electrons in the elementary reaction step and F is the Faraday constant.

Typical examples of the Cottrell plot of the data obtained at the temperature below the melting point of the electrolyte are presented in Fig. 2b, c. For times shorter than 1 s they are linear with a non-zero intercept. At longer times the slope of the plot increases and then decreases (Fig. 2b). Finally the plot becomes approximately linear with intercept close to zero. Also it was observed that the lower the temperature the longer is the time taken for deviation from linearity of the Cottrell plot to occur (Fig. 2b, c). This effect can be caused by the change of the reactant transport mode from radial to linear diffusion. The zero intercept of the Cottrell plot for long times (Fig. 2b) and the peak-shaped slow scan rate cyclic voltammogram support this conclusion. The extrapolation of the short time linear part of the Cottrell plot to infinity gives the value of I_1 and the value of D_{app} near the electrode surface [16, 17]. One has to remember that in the case of the standard size electrodes restricted diffusion can affect the Cottrell plot in a similar way [21, 22]. Such an interpretation was earlier proposed for frozen electrolytes containing redox-active ions and molecules [4–6]. This is also possible in the studied case.

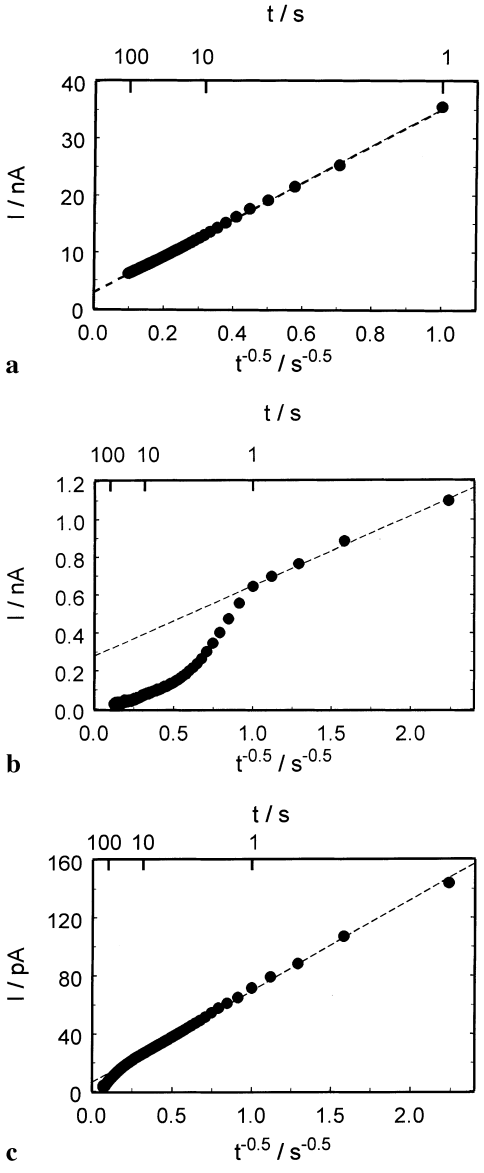

Fig. 2a–c Plot of the anodic current (I) against reciprocal of square root of time ($t^{-1/2}$) (Cottrell plot) obtained from the potential step (0.1–0.9 V) experiments in 0.002 M $Fc(CH_2OH)_2$ in TBACl30 at Pt microelectrode (d = 20 μm), at temperatures **a** 300 K, **b** 255 K and **c** 230 K. The *dashed lines* are linear regression lines

Examples of the temperature dependence of D_{app} on the reciprocal of temperature (T) are presented in Figs. 3 and 4. The shape of this dependence is generally similar for all systems studied. The observed dependence is approximately linear at temperatures above the melting point of the electrolyte. The region of linearity extends about 20 K below the melting point of the electrolyte. At lower temperature the slope of the Arrhenius plot increases about three- to four-fold. This indicates slower reactant transport towards the electrode surface. The observed behaviour is somewhat different from that

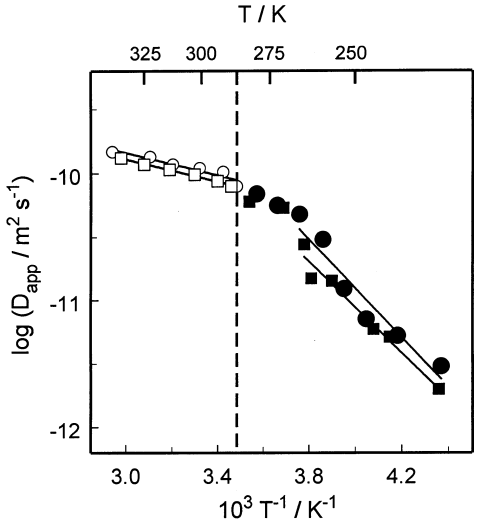

Fig. 3 Plot of the logarithm of the apparent diffusion coefficient (D_{app}) of $Fc(CH_2OH)_2$ (■) and $Ru(NH_3)_6^{3+}$ (●), against reciprocal of temperature (T^{-1}) in TBACl30. *Empty* and *solid symbols* mark D_{app} values at temperatures above and below the melting point of the electrolyte. *Vertical long dashed line* marks melting point of electrolyte

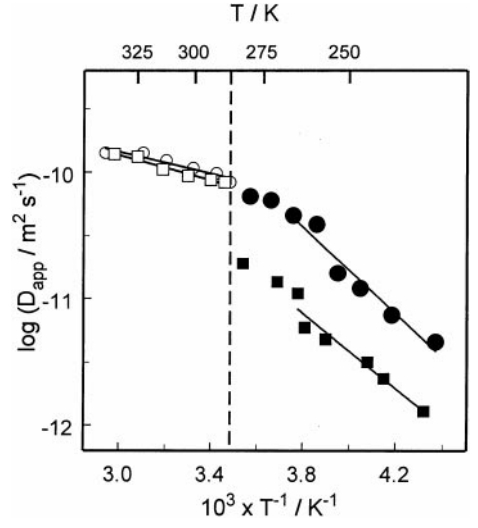

Fig. 4 Plot of the logarithm of apparent diffusion coefficient (D_{app}) of $Fe(CN)_6^{3-}$ in the presence (●) and absence (■) of K^+ ions, against reciprocal of temperature (T^{-1}) in TBACl30. *Empty* and *solid symbols* mark D_{app} values at temperatures above and below the melting point of electrolyte. *Vertical long dashed line* marks melting point of electrolyte

observed for $Fe(CN)_6^{3-}$ ions in tetramethylammonium fluoride [4] and hydroxide hydrates [6]. In these electrolytes the change of the slope occurs at a temperature very close to the melting point of the electrolyte and the slope is halved [4, 6, 8].

It is also interesting that change of the cation in the $Fe(CN)_6^{3-}$ salt from K^+ to the cation of the electrolyte, namely TBA^+, causes a considerable decrease in D_{app} at temperatures below the melting point of the electrolyte (Fig. 4). On the other hand, no substantial difference is observed in D_{app} of a $Ru(NH)_6^{3+}$ redox system when $Ru(NH)_6Cl_3$ was present in electrolytes with different anions: Cl^- in TBACl30 and Br^- in TBABr32.

Impedance of the cell Au|$K_3Fe(CN)_6$ and $K_4Fe\ (CN)_6$, *TBAXn*|Au

Reaction 1 was also studied by impedance spectroscopy at temperatures above and below the melting point of the electrolyte. The stability of both redox-active ions involved in this reaction allows experiments in a two-electrode cell, which is useful in the case of low conductivity of the electrolyte. Analogous experiments have been previously performed with the same redox system in $(CH_3)_4NF \cdot 4H_2O$ (TMAF4) [5].

The example of impedance spectra obtained at temperatures above the melting point of the electrolyte is presented in Fig. 5. In a Nyquist representation, the high-frequency part of the spectrum consists of a slightly depressed semicircle. The low-frequency part consists of a straight line with slope unity. This indicates that in liquid electrolyte at some frequency the electron exchange between reactant and electrode becomes the rate-determining step [23]. The fact that the best fit equivalent circuit is that proposed by Randles [23] confirms this conclusion. The charge-transfer resistance (R_{ct}) is 9.5 Ω cm^2, indicating moderately fast electron transfer. It is known from the literature that reaction 1 is relatively fast [24, 25]. However, adsorption of TBA^+ cations on the electrode surface may decrease the rate of heterogeneous electron transfer as observed with other electrochemical redox reactions [19, 26]. This may also be true in the case studied.

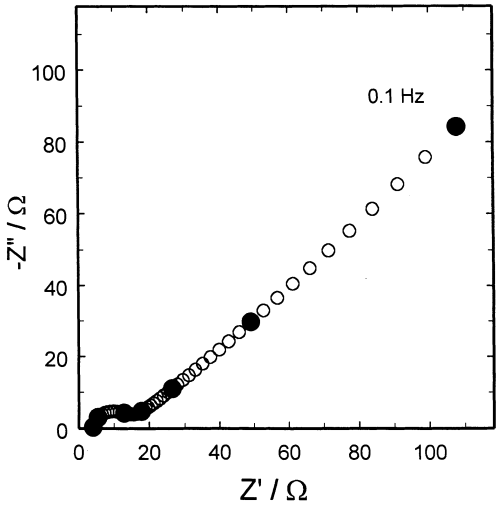

Fig. 5 Impedance spectrum of the cell Au | 0.003 M $K_3Fe(CN)_6$ and $K_4Fe(CN)_6$ (1 : 1), TBACl30 | Au obtained at a temperature above the melting point of the electrolyte (293 K). The frequency difference between points marked by *larger filled symbols* is equal to one order of magnitude

The electrode electrolyte interface is represented by constant phase element (CPE). Its impedance can be defined as

$$Z_{CPE} = 1/C(j\omega)\phi \quad (5)$$

where $j = (-1)^{0.5}$ and ω is an angular frequency. The value of parameters C and ϕ are $(2 \pm 2) \times 10^{-10}$ F m^{-2} and 0.90 ± 0.05 respectively. The value of the factor C is one order of magnitude lower than that observed for polycrystalline Au electrodes in non-adsorbing aqueous electrolytes [27, 28]. This may indicate the adsorption of TBA^+ cations suggested above. The character of the impedance spectrum is different from that in the case of liquid TMAF4 or $(CH_3)_4NOH \cdot 5H_2O$ (TMAOH5) [5, 6], where reaction 1 is entirely controlled by reactant transport towards the electrode surface [5]. The concentration of salt in stoichiometric tetrabutylammonium hydrates is much smaller than in tetramethylammonium fluoride or hydroxide hydrates. Therefore diffusion of redox-active ions in liquid electrolyte is not expected to be hindered as was observed in TMAF4, which in the liquid state is a concentrated 6.2 M aqueous solution [4]. The observed different behaviour of reaction 1 in tetrabutylammonium halide hydrates seems to be a result of a slowing down of the heterogenous electron transfer by adsorbed TBA^+ cations and fast diffusion of reactants towards the electrode surface.

At temperatures below the melting point of the electrolyte, the shapes of the impedance spectra are different from those observed in liquid electrolyte (Fig. 6). The increase in the slope of the Nyquist plot at the lowest frequencies is the most striking feature. A similar effect was also observed in the case of the same redox system in frozen TMAF4 [5]. The value of the onset frequency (f_{onset}), where the slope of the plot becomes larger than unity, depends on temperature: the lower temperature the lower the f_{onset}. The observed change in the low-frequency part of the impedance spectrum may indicate restriction of the volume accessible for redox-active ions to the limited space near the electrode surface [29–32]. This also confirms the suggestion made above that the slope change on Cottrell plots (Fig. 2) is at least partially caused by this effect. The semicircle observed in the high-frequency part of the spectrum is more depressed and deformed than that obtained at temperatures above the melting point, but the reason for this behaviour is unclear.

The electrical conductivity (σ) of the studied electrolytes containing redox-active ions was estimated using the values Z' extrapolated from the high-frequency part of the Nyquist plot to $Z'' = 0$. It is clear that addition of $Fe(CN)_6^{4-}$ and $Fe(CN)_6^{3-}$ ions affects the temperature dependence of σ (Fig. 7). The effect is similar in all tetrabutylammonium halide hydrates [4]. The substantial increase in conductivity at a temperature of about 20 K below the melting point is the most important effect of the addition of redox-active ions to tetrabutylammonium halide hydrates similarly to previous observations [4, 6].

In order to check whether the heterogeneous nature of frozen electrolyte containing redox-active ions can be considered as the reason for the increase of the slopes of the impedance spectra at low frequencies, we performed impedance spectroscopy experiments in a two-electrode cell filled with spherical particles of hydrophobic silica together with aqueous electrolyte solution containing $Fe(CN)_6^{3-}$ and $Fe(CN)_6^{4-}$. In this model system, beads represent frozen electrolyte crystals impenetrable for redox-active ions. The corresponding impedance spectrum is presented on Fig. 8. The slope of the Nyquist plot at low frequencies is much greater than unity as

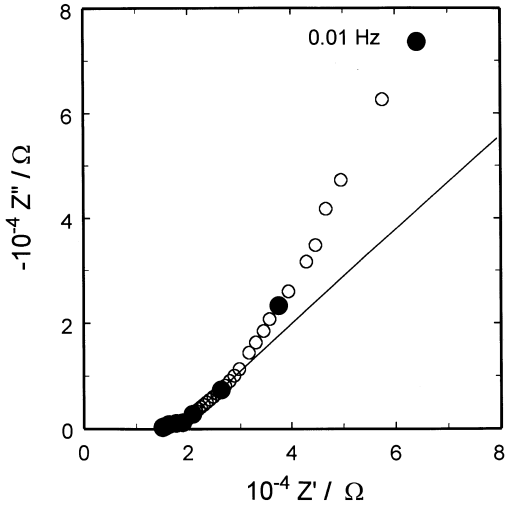

Fig. 6 Impedance spectrum of the cell Au | 0.003 M $K_3Fe(CN)_6$ and $K_4Fe(CN)_6$ (1 : 1). TBACl30 | Au obtained at a temperature below the melting point of the electrolyte (263 K). The frequency difference between points marked by *larger filled symbols* is equal to one order of magnitude. The slope of the solid line is equal to unity

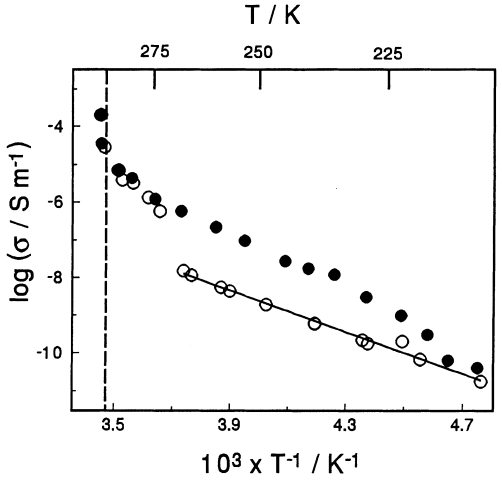

Fig. 7 Plot of the logarithm of conductivity (σ) of TBACl30 (○) and the same electrolyte containing 0.002 M $K_3Fe(CN)_6$ and $K_4Fe(CN)_6$ (●) against reciprocal of temperature (T^{-1}). *Long dashed vertical* line marks melting point of electrolyte

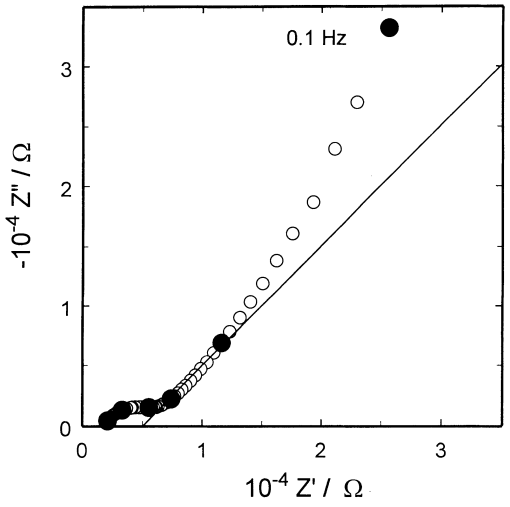

Fig. 8 Impedance spectrum of the cell Au | 0.001 M $K_3Fe(CN)_6$ and $K_4Fe(CN)_6$ (1 : 1), TBACl30, RP–18 | Au obtained at a temperature above the melting point of the electrolyte (298 K). The frequency difference between points marked by *larger filled symbols* is equal to one order of magnitude. The slope of the *solid line* is equal to unity

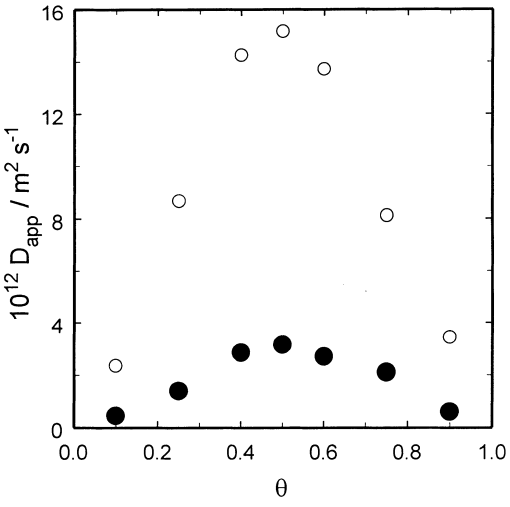

Fig. 9 Plot of the average apparent diffusion coefficient (D_{app}), of $Fe(CN)_6^{3-}$ and $Fe(CN)_6^{4-}$ ions at 260 K (■) and 248 K (●) against the fraction of $Fe(CN)_6^{3-}(\theta)$ in frozen TBACl30

expected for restricted diffusion [29–32]. The result of this experiment supports the conclusion that reactant transport occurs through the intergrain space of the frozen electrolyte.

It is also interesting to investigate whether the oxidized and the reduced components of the redox system are transported towards the electrode surface at the same rate. This is obvious in liquid electrolyte but not necessarily true in solid electrolytes [32, 33]. For this purpose the impedance experiments were performed in a two-electrode cell filled with frozen electrolyte with different ratios of $K_3Fe(CN)_6$ and $K_4Fe(CN)_6$. The rate of transport to the electrode surface can be related to the impedance of semi-infinite diffusion towards the electrode surface, the so-called "Warburg impedance" (Z_W). This can be described by the following equation:

$$Z_W = [RT/(2\omega)^{0.5}A(nF)^2] \times (1/c_{ox}D_{ox} + 1/c_{red}D_{red}) \times (1 - j) \quad (6)$$

where ω is an angular frequency, A the electrode surface area, and c_{ox}, D_{ox}, c_{red}, D_{red} are concentrations and diffusion coefficients of oxidized and reduced form of reactant respectively. At temperatures below the melting point of the electrolyte, at moderate frequencies, the Nyquist plot is linear with a slope equal to unity. This means that at this frequency range (1–10 Hz in the case presented in Fig. 6) the overall impedance of the studied cell is dominated by Z_W. Replacing c_{ox} and c_{red} with $c_{eff} = c_{ox} + c_{red}$ and assuming that the effective diffusion coefficient (D_{eff}) is equal D_{ox} and D_{red} one may calculate the latter parameter from the value of Z_W. The plots of the values of D_{eff} against the fraction of the oxidized form of the redox reactant, θ, ($\theta = c_{ox}/(c_{ox} + c_{red})$ at two selected temperatures below the melting point of the electrolyte are presented on Fig. 9. The obtained plot passes through a maximum at $\theta = 0.5$, indicating that the two components of the redox systems are transported towards the electrode surface at the same rate.

Discussion

Although almost all results presented in this paper were obtained in TBACl30, the others obtained in TBAF32 and TBABr32 are similar qualitatively and quantitatively.

One may conclude that the electrochemical redox reactions 1–3 occur also over a limited temperature range below the melting point of tetrabutylammonium halide hydrates. This behaviour is similar for all studied reactions and electrolytes. Freezing of the electrolyte affects some features of the transport of reactants. The effects connected with restricted diffusion observed in chronoamperometry and impedance spectroscopy experiments are similar to those previously observed for reaction 1 in frozen tetramethylammonium fluoride and hydroxide hydrates [4, 5]. It was suggested previously that the motion of the redox-active ions is restricted to the intergrain space of the polycrystalline electrolyte [4, 5]. It seems that this is also the case for the systems studied. The lack of any substantial change in D_{app} (with one exception discussed later) at temperatures near the melting point of the electrolyte may indicate a similar mechanism of reactant transport in liquid and frozen electrolyte, namely physical diffusion. The symmetry of the composition dependence of D_{app} may also indicate the same mechanism of the transport process. Therefore one may conclude that reactant transport occurs by diffusion through the intergrain space of the electrolyte. The similarity of the impedance spectra obtained in frozen electrolyte and in model heterogeneous system supports this conclusion. A contribution of migration to

Table 1 The activation energies (E_a) of transport of reactants in liquid and frozen TBACl30 containing redox-active ions and molecules

Reactant	E_a/eV	
	Liquid	Frozen[c]
$Fe(CN)_6^{3-}$ [a]	0.15 ± 0.02	0.64 ± 0.07
$Fe(CN)_6^{3-}$ [b]	0.19 ± 0.04	0.61 ± 0.08
$Ru(NH_3)_6^{3+}$	0.15 ± 0.03	0.69 ± 0.09
$Fc(CH_2OH)_2$	0.17 ± 0.02	0.64 ± 0.08

[a] $Fe(CN)_6^{3-}$ introduced as $K_3Fe(CN)_6 \cdot 3H_2O$
[b] $Fe(CN)_6^{3-}$ introduced as $TBA_3Fe(CN)_6$
[c] At temperatures below 265 K

the transport process is possible, but this is difficult to estimate because of the lack of knowledge about the composition of the intergrain space of the electrolyte. Similar values of D_{app} and similar shapes of the temperature dependence of this parameter for all the systems studied indicate that the transport of the reactant is independent of the type of frozen electrolyte.

The rate transport of reactants towards the electrode surface depends more strongly on temperature at temperatures at least 20 K below the melting point (Figs. 3 and 4). It is interesting that the change of slope of the temperature dependence of E^0 of the redox systems studied occurs at approximately the same temperature for each system [7]. As E^0 is sensitive to reactant environment, one may conclude that at a temperature about 20 K below the melting point the local environment of the reactants changes, thereby also affecting the rate of their motion.

The activation energies of the transport process (E_a) can be obtained from the following equation:

$$D_{app} = D_o \exp(-E_a/kT) \quad (7)$$

The values of E_a are presented in Table 1. They are similar to those obtained in the case of reaction 1 in frozen tetramethylammonium fluoride and hydroxide hydrates (0.66–0.70 eV). They are also similar to those of Fe^{3+} and Fe^{2+} hydrated ions in $HClO_4 \cdot 5.5\ H_2O$ [2]. One may conclude that, for the systems studied so far, E_a in a frozen electrolyte is generally independent of the redox system and the electrolyte. The larger change of E_a upon freezing of tetrabutylammonium halide hydrates is due to the lower activation energy for diffusion in diluted electrolyte media such as TBACl30 in comparison to that in a concentrated electrolyte such as TMAF4 or TMAOH5. The decrease in D_{app} and increase in E_a upon freezing may be caused by the different composition and the greater rigidity of the immediate environment of the redox reactants. It obviously causes a larger hindrance to the motion of the redox reactant. Also, the volume in which the ions can move is restricted, and eventually they cannot move in every direction. The net motion is slower than in a liquid electrolyte and causes the decrease in the observed values of D_{app}. The observed decrease in the value of D_{app} for $Fe(CN)_6^{3-}$ ions in the absence of K^+ at a temperature close to the melting point may be the result of a partial incorporation and immobilization of $Fe(CN)_6^{3-}$ ions together with TBA^+ cations into electrolyte grains during the freezing process. At a given temperature the values of D_{app} in frozen tetrabutylammonium halide hydrate are about one order of magnitude larger than those in frozen tetramethylammonium cation hydrates [4, 6]. One has to remember that two opposite effects may affect the estimated D_{app} value in frozen electrolyte. Adsorption of TBA^+ cations on the electrode surface causes a current decrease, leading to the underestimation of D_{app}. On the other hand this parameter is obtained from the current recorded during a relatively short time corresponding to restriction of the diffuse layer to the volume close to the electrode. If the model proposed for frozen electrolyte containing redox-active ions or molecules [5, 6] is valid the reactant concentration is greater than in the bulk of electrolyte. The shape of the I vs $t^{-0.5}$ dependence (Fig. 2b) indicates that this is the case. In some cases D_{app} can be overestimated by one order of magnitude.

One may argue that the value of D_{app} obtained describes the mobility of redox-active ions and molecules in the thin layer near the electrode surface. The obtained chronoamperometry and impedance data indicate that the concentration gradient extends further into the electrolyte. The change of electrical conductivity of the electrolyte after addition of redox-active ions (Fig. 7) indicates that they induce changes in the bulk of the electrolyte and not only near the electrode surface. However it is possible that the higher mobility of ions and molecules near the electrode surface can be caused by so-called surface premelting. This phenomenon is observed at the ice solid interface [34, 35]. The temperature at which surface premelting starts is decreased by the presence of impurities. In our case redox-active compound added to stoichiometric hydrate can be considered as impurity which may eventually cause premelting. Unfortunately we could not find in the literature any data about premelting of electrolytes.

Acknowledgements The author thanks Prof. Zofia Borkowska for helpful comments on this manuscript. The technical assistance of Ms Elzbieta Wojtaszek in experiments with model system is gratefully acknowledged.

References

1. Matsunaga A, Itoh K, Fujishima A (1986) J Electroanal Chem 205: 125
2. Borgeding A, Brost E, Schmickler W, Dinan T, Stimming U (1990) Ber Busenges Phys Chem 94: 607
3. Opallo M (1995) J Electroanal Chem 399: 169
4. Opallo M (1996) J Electroanal Chem 411: 145
5. Opallo M (1996) J Electroanal Chem 418: 91
6. Opallo M (1998) J Electroanal Chem 446: 187
7. Opallo M (1998) J Electroanal Chem 446: 39
8. Borkowska Z, Opallo M, Tymosiak-Zielinska A, Zoltowski P (1998) Colloids & Surfaces. A: Physicochemical and Engineering Aspects 134: 63

9. Jeffrey GA, McLean WJ (1967) J Chem Phys 47: 414
10. Dyadin YuA, Udachin KA (1984) J Incl Phenom 2: 61
11. Opallo M, Tymosiak-Zielinska A, Borkowska Z (1997) Solid State Ionics 97: 247
12. Nolte RE, Pletcher D (1990) J Electroanal Chem 293: 273
13. Ives DJG, Janz GJ (1961) Reference electrodes, theory and practise. Academic, New York, p 358
14. Ashraf-Khorassani M, Braun RD (1987) Corrosion 43: 32
15. Piela P, Wrona PK, Galus Z (1994) J Electroanal Chem 378: 159
16. Wightman RM, Wipf DO (1989) In: Bard AJ (ed) Electroanalytical chemistry, vol 15. Dekker, New York, p 89 and references therein
17. Denault G, Mirkin MV, Bard AJ (1991) J Electroanal Chem 308: 27
18. Beriet C, Pletcher D (1993) J Electroanal Chem 361: 93
19. Wandlowski T, de Levie R (1995) J Electroanal Chem 380: 201
20. Lindenbaum S, Boyd SE (1964) J Phys Chem 68: 911
21. Oglesby DM, Omang SH, Reilley CN (1965) Anal Chem 37: 1312
22. Aoki K, Tokuda K, Matsuda H, Oyama N (1984) J Electroanal Chem 176: 139
23. Randles JEB Disc Faraday Soc (1947) 1: 11
24. Campbell SA, Peter LM (1994) J Electroanal Chem 364: 254
25. Winkler K (1995) J Electroanal Chem 381: 151
26. Fawcett WR, Fedurco M, Opallo M (1992) J Phys Chem 96: 9959
27. Fawcett WR, Kovacova Z, Motheo AJ, Foss Jr CA (1992) J Electroanal Chem 326: 91
28. Piela B, Wrona PK (1995) J Electroanal Chem 388: 69
29. Franceschetti DR, Mac Donald JR (1982) J Electrochem Soc 127: 343
30. Rubinstein I, Rishpon J, Gottesfeld S (1986) J Electrochem Soc 133: 729
31. Gabrielli C, Takenouti H, Haas O, Tsukada A (1991) J Electroanal Chem 302: 59
32. Sharp M, Lindholm-Sethson B, Lind EL (1993) J Electroanal Chem 345: 223
33. Kupis D, Ochmanska J, Galus Z (1992) Pol J Chem 66: 1789
34. Nenov D, Trayanov A (1989) Surf Sci 213: 388 and references therein
35. Beaglehole D, Wilson P (1994) J Phys Chem 98: 8096 and references therein